

Characteristics of Linearly-Forced Scalar Mixing in Homogeneous, Isotropic Turbulence

Phares L. Carroll*, Siddhartha Verma**, and G. Blanquart*
Corresponding author: plcarroll@caltech.edu

* Department of Mechanical Engineering, ** Graduate Aerospace Laboratories
California Institute of Technology

Abstract: To realize the potential of Direct Numerical Simulation (DNS) in turbulent mixing studies, it is necessary to develop numerical schemes capable of sustaining the physics of both the velocity and scalar fields, without altering the inherent isotropy and homogeneity of turbulence. Further, the physics must be maintained for a time sufficient to allow for meaningful data to be obtained. In this work, a scheme to sustain the physics of a decaying turbulent scalar field is presented, and it is shown to recover the appropriate scalar energy spectrum for all Schmidt numbers investigated. The physical significance and statistical qualities of this forcing technique are contrasted with those of the widely-accepted mean scalar gradient forcing scheme. This proposed scalar field forcing will find application in simulation studies of the decay of passive scalar quantities subject to turbulent flow environments.

Keywords: Direct numerical simulation, scalar field forcing techniques, turbulent mixing.

1 INTRODUCTION AND MOTIVATION

A passive scalar is a quantity in a flow that can be convected and diffused without impacting the overall flow dynamics. The mixing of passive scalars in turbulent flows is an active area of research, which finds applications in a broad range of fields, such as combustion, atmospheric flow dynamics, and oceanographic flows. Direct Numerical Simulation (DNS) studies of passive mixing often use forced velocity and scalar fields to prevent the turbulent fields from decaying, thereby maximizing the accessible Taylor-Reynolds number (Re_λ) and Schmidt number (Sc), the ratio of viscous diffusion to mass diffusion. To ensure the results obtained in such DNS studies are representative of the physics of passive scalar mixing, and not a manifestation of the numerical schemes implemented, the forcing methods used must preserve the statistics of turbulence at all wavenumbers and have minimal impact on the physics of the dynamically important scales.

In the context of simulations of turbulent flows, passive scalars can be either forced, where energy is continuously injected into them, or they can decay, where energy is not provided after its initial injection. The most commonly used means for sustaining a scalar field in DNS studies involves forcing the standard advection-diffusion equation proportional to an applied mean gradient [1, 2]. Forcing with a mean gradient corresponds physically to supplying energy continuously to the scalar field, replenishing any losses. The current work endeavors, instead, to create a framework in which the decay of a scalar quantity can be statistically sustained, such as would be encountered in decaying grid turbulence. In grid turbulence, a grid is forced through a fluid, inducing turbulence and providing energy to the flow. Once the grid has passed, there is no energy provided to the scalar field; it will decay, and, after an initially transient period, it will enter a self-similar flow regime. In order to facilitate simulation studies of scalar field decay, a new method for driving the scalar field to stationarity is needed. Such a methodology is proposed and evaluated. The proposed forcing scheme uses the scalar variance as a parameter in the source term appended to the advection-diffusion equation. It will be shown that the statistical and energy spectrum characteristics of

this scalar variance forcing are representative of a decaying scalar quantity. This scheme is examined over a range of relatively low Taylor-Reynolds and Schmidt numbers. Additionally, this work provides commentary on the characteristics and limitations of the mean scalar gradient forcing method.

2 DESCRIPTION OF SIMULATION STUDY

A primary objective of this study is to evaluate the characteristics of the proposed scalar variance forcing technique in homogeneous, isotropic turbulent flow over a range of physically-relevant Schmidt numbers. This requires that both the velocity and scalar governing equations evolve to stationarity. The velocity field is forced to maintain a suitable Re_λ , while the scalar field is forced with both the proposed method and the mean scalar gradient method to allow for a comparison. This study covered Taylor-Reynolds numbers, $Re_\lambda = [30, 55, 140]$, and Schmidt numbers, $Sc = [1, 4, 16, 64]$. From the data generated in the performed simulations, the associated scalar energy spectra were calculated along with appropriate statistical metrics of isotropy and homogeneity. The specific simulation parameters and pertinent fluid properties are included in Table 1. The last two columns are indicative of the resolution of the simulations, where κ_{max} corresponds to the maximum wavenumber accessible in the simulation, η is the Kolmogorov lengthscale, and η_b is the Batchelor lengthscale, defined as $\eta_b = \eta Sc^{-\frac{1}{2}}$. The Kolmogorov and Batchelor lengthscales indicate the smallest lengths for which the governing equations must be solved for the velocity and scalar fields, respectively.

Run No.	Re_λ	Sc	N^3	ν	D	$\kappa_{max}\eta$	$\kappa_{max}\eta_b$
1	30	1	64^3	0.02	0.02	1.50	1.50
2	30	4	128^3	0.02	5.0×10^{-3}	2.94	1.47
3	30	16	384^3	0.02	1.25×10^{-3}	8.73	2.18
4	55	1	128^3	2.8×10^{-3}	2.8×10^{-3}	1.48	1.48
5	55	4	192^3	2.8×10^{-3}	7.0×10^{-4}	2.20	1.10
6	55	16	384^3	2.8×10^{-3}	1.75×10^{-4}	4.28	1.07
7	55	64	512^3	2.8×10^{-3}	4.375×10^{-5}	5.80	0.725
8	140	1	512^3	2.8×10^{-3}	2.8×10^{-3}	1.74	1.74

Table 1: Simulation parameters for the DNS study conducted. The column headings, Re_λ , Sc , N , ν , and D , are the Taylor-Reynolds number, Schmidt number, simulation size, fluid kinematic viscosity, and scalar diffusivity, respectively. Note that runs 5-7 are not fully resolved and, hence, cannot be termed DNS runs. Support for the validity of results obtained from these slightly under-resolved simulations will be provided in section 4.1.

Conventional wisdom mandates highly restrictive resolution requirements for both the velocity and scalar fields when performing DNS studies. The accepted resolution limit for the velocity field is $\kappa_{max}\eta \geq 1.5$ [3]. The resolution limit for the scalar field is more severe. To ensure the accuracy of calculated second-order scalar statistics, the resolution limit is $\kappa_{max}\eta_b \geq 1.5$, while it is pushed upward to $\kappa_{max}\eta_b \geq 3.0$ to guarantee accuracy of fourth-order scalar statistics [4]. Thus, increasingly higher-order scalar statistics require an increasingly restrictive $\kappa_{max}\eta_b$. Consequently, the larger the Sc , the more difficult it becomes to satisfy these guidelines. One unfortunate result of this is that simulation studies are restricted to low-Schmidt numbers. Once the Schmidt number becomes on the order of 10^3 , where some physically-relevant scalar transport occurs, simulations become too expensive computationally to perform. It will be argued briefly in section 4.1 that it is possible to relax the resolution restriction on the scalar field, while incurring only minimal error in the resulting calculations. This argument will only apply to simulations 5-7 in Table 1, for which the scalar fields are slightly unresolved ($\kappa_{max}\eta_b = 1.1, 1.07, 0.725 \leq 1.5$).

2.1 HOMOGENEOUS ISOTROPIC TURBULENCE (HIT)

Homogeneous isotropic turbulence (HIT) has stringent statistical requirements. First, both the velocity and scalar fields must be symmetrically distributed. Symmetry will manifest in a vanishing skewness for both the velocity and scalar, where skewness is defined as the third moment of the variable of interest.

Second, the scalar and velocity fields must be isotropic. For the scalar, isotropy is associated with equal averaged-scalar fluxes: $\langle u'Z \rangle = \langle v'Z \rangle = \langle w'Z \rangle$. The requirement of reflectional symmetry of the Navier-Stokes equations additionally restricts these scalar fluxes to be zero. For the velocity, isotropy corresponds to a diagonal Reynolds stress tensor, where the averaged-Reynolds stresses tend to zero and the variances tend to equivalence: $\langle u'v' \rangle = \langle u'w' \rangle = \langle v'w' \rangle = 0$ and $\langle u'^2 \rangle = \langle v'^2 \rangle = \langle w'^2 \rangle$. Lastly, the velocity forcing must produce the desired spectral trend, as shown in Fig. 1. The length scales of a turbulent flow are partitioned into the energy containing, energy transferring (the inertial subrange), and energy dissipating scales. The key trend to be captured by the numerical scheme adopted for the velocity field is the $-\frac{5}{3}$ slope in the inertial sub-range. For the scalar field, the appropriate scaling in the inertial sub-range is more subtle, as it is a function of the Taylor-Reynolds number, Re_λ , and the Schmidt number, Sc .

2.2 FORCING THE VELOCITY FIELD

There are two broadly-accepted ways of forcing the velocity field in numerical studies. The first is to force the velocity field proportional to the magnitude of the velocity fluctuations themselves, as proposed by Lundgren [10]. This linear forcing scheme has the advantages of being straightforward to implement and applicable to non-spectral codes. The second is to force the velocity field in spectral space. This type of forcing is more complex, but it allows for more precise control over the location of the forcing operation.

Prior to analyzing the scalar forcing, the schemes used to force the velocity field towards statistical stationarity were examined to determine if they were producing a homogeneous and isotropic turbulent field. This investigation was warranted by the coupling between the (unforced) momentum and advection-diffusion equations,

$$\frac{\partial \mathbf{u}}{\partial t} + \mathbf{u} \cdot \nabla \mathbf{u} = -\nabla \left(\frac{p}{\rho} \right) + \nu \nabla^2 \mathbf{u} \quad (1)$$

$$\frac{\partial Z}{\partial t} + \mathbf{u} \cdot \nabla Z = D \nabla^2 Z. \quad (2)$$

Here, u , p , ρ , ν , Z , and D are the fluid velocity, hydrodynamic pressure, density, kinematic viscosity, the scalar quantity of interest, and molecular diffusivity. Turbulence is inherently a non-linear phenomenon, but the advection-diffusion equation itself is linear with respect to the scalar quantity, and, therefore, cannot produce a turbulent scalar field. Instead, turbulence is generated first by the non-linear convective term in the momentum equation, and, then, enters into the scalar field via the scalar flux term ($\mathbf{u} \cdot \nabla Z$). Thus, it is pivotal to implement a sound velocity forcing to create the desired statistics for HIT and to couple properly turbulence to the scalar field.

In this work, the velocity field is forced using both methods to facilitate a comparison between them. Initially, the velocity field was forced linearly according to Lundgren's proposed form,

$$\frac{\partial \mathbf{u}}{\partial t} + \mathbf{u} \cdot \nabla \mathbf{u} = -\nabla \left(\frac{p}{\rho} \right) + \nu \nabla^2 \mathbf{u} - Q \mathbf{u}, \quad (3)$$

where Q is a constant and \mathbf{u} is a vector of the fluctuating velocity components. Then, the velocity field was forced spectrally using only a small number of modes, which are clustered about a single waveshell [5]. This spectral forcing, \mathbf{f} , is determined by geometrical constraints. The dot product of the velocity fourier coefficients ($\hat{\mathbf{u}}$) with the wavevector, \mathbf{k} , must vanish in order to satisfy incompressibility,

$$\mathbf{k} \cdot \hat{\mathbf{u}} = 0. \quad (4)$$

To ensure that the forcing is orthogonal to the velocity field, and, hence, is not altering the velocity field

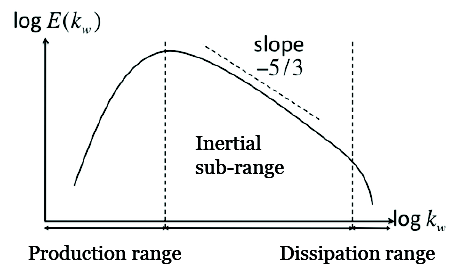


Figure 1: Energy cascade trending in spectral space.

statistics directly, the dot product of the forcing term and the velocity fourier coefficients must vanish,

$$\hat{\mathbf{u}} \cdot \mathbf{f} = 0. \quad (5)$$

These two conditions ensure mutual orthogonality of the forcing and the local velocity components. Finally, two random phase angles, θ_1 and θ_2 , are introduced to maintain isotropy,

$$\mathbf{f} = \|\mathbf{f}\| \cdot \hat{\mathbf{e}}_f \cdot \exp(i(\theta_2 - \theta_1)). \quad (6)$$

The waveshell magnitudes for which the forcing was applied was $2 \leq \kappa_f \leq 4$. A relative weight was assigned to each waveshell magnitude based on its location with respect to a Gaussian centered about $\kappa_f = 3$. This narrow distribution would reduce any impact on the small scales of the flow and would further distribute the injected energy over a physically-appropriate range of large-scale structures.

With the data obtained from these two velocity forcing techniques, the kinetic energy spectrum resulting from each was calculated. These are provided in Fig. 2. The theoretically-predicted scaling of $E(\kappa) \sim \kappa^{-5/3}$ [6] is clearly present in the inertial sub-range of the spectrally-forced velocity field. Although, when the linear forcing was used, the scaling derived was described more accurately as $E(\kappa) \sim \kappa^{-4/3}$.

The probability density function (PDF) for the Reynolds stresses and variances produced by these forcing techniques were also calculated and averaged over three eddy-turnover times, τ_{eddy} . They are depicted in Fig. 3 and Fig. 4. The requirements for a HIT velocity field are isotropy, homogeneity, and symmetry. By observation of Fig. 3 and Fig. 4, it is apparent that the spectral velocity forcing clearly satisfies the criteria for HIT; however, the linear velocity forcing is not as strongly isotropic.

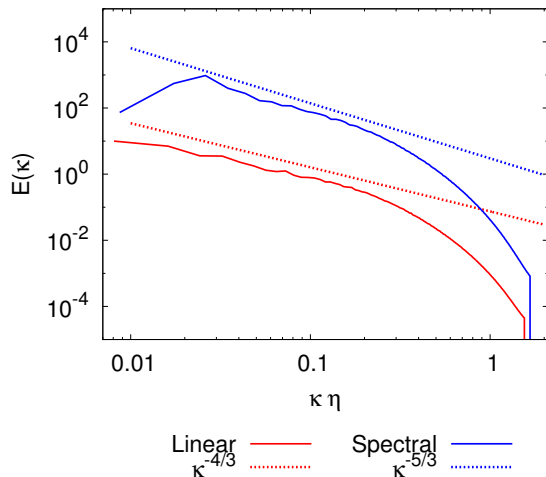


Figure 2: 3-D kinetic energy spectrum generated by the linear ($N = 384^3, Re_\lambda = 120$) and spectral ($N = 512^3, Re_\lambda = 140$) velocity forcing schemes.

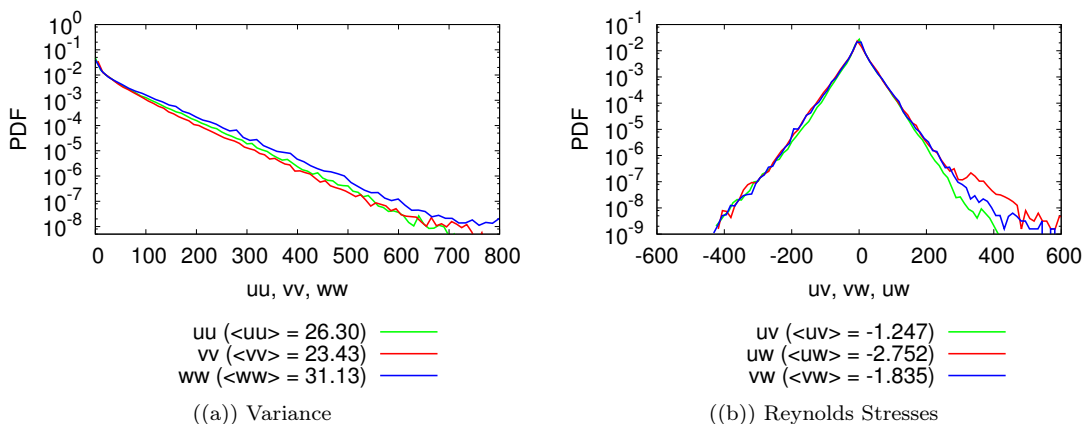


Figure 3: PDF of stress tensor quantities for linear velocity forcing ($N = 384^3, Re_\lambda = 120, Sc = 1$).

As the velocity and scalar equations are tightly coupled, it is possible that the use of a linear velocity forcing may corrupt the proper development of the scalar field both due to its non-ideal statistical properties

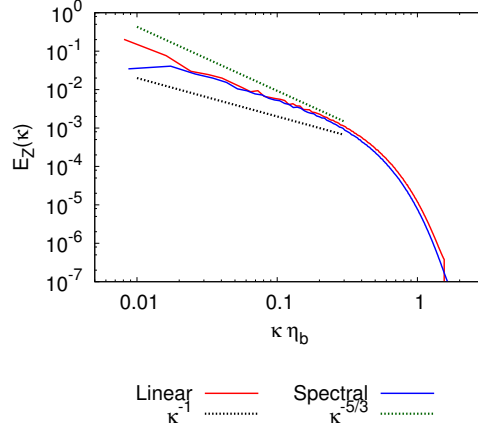


Figure 5: 3-D scalar energy spectrum generated when the scalar field is forced via a mean scalar gradient and the velocity field is forced by the linear ($N = 384^3, Re_\lambda = 120, Sc = 1$) and spectral ($N = 512^3, Re_\lambda = 140, Sc = 1$) methods.

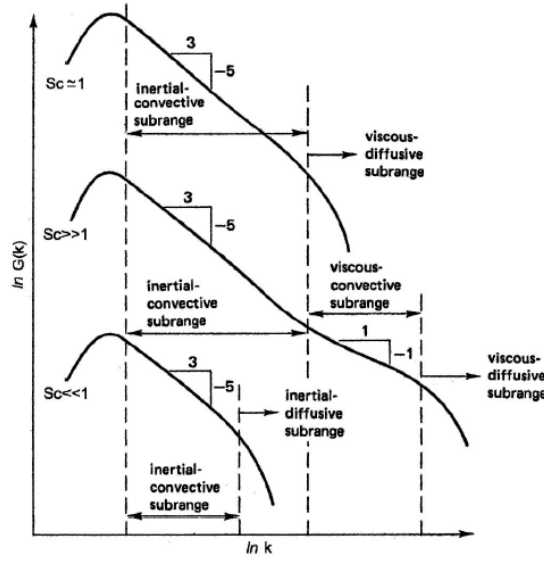


Figure 6: Scalar spectrum ($G(\kappa)$) scaling with wavenumber (κ) [7].

3.1 Standard Mean Scalar Gradient Forcing

A statistically stationary scalar field is often generated with a standard mean scalar gradient forcing,

$$\frac{\partial Z}{\partial t} + \mathbf{u} \cdot \nabla Z = D \nabla^2 Z - G \cdot \mathbf{u}, \quad (7)$$

where G is a mean scalar gradient and D is molecular diffusivity. Another motivating factor for the development of the proposed forcing was the desire to improve on the scalar field statistics that are produced when the scalar field is forced with a mean gradient.

As indicated in Fig. 7, the PDFs of the scalar fluxes generated by a mean scalar gradient method are indicative of significant anisotropy; the scalar flux component $\langle uZ \rangle$ is always strongly non-zero. Two of the scalar fluxes ($\langle vZ \rangle$ and $\langle wZ \rangle$) assume an average value of zero, but the streamwise scalar flux term will never vanish. The impacts of this anisotropy can be understood by examining the derivation of the mean scalar gradient forcing. Beginning with the forced advection-diffusion equation, Eq. 7, and multiplying by

the scalar fluctuation, Z , results in Eq. 8,

$$\frac{\partial(\frac{1}{2}Z^2)}{\partial t} + \nabla \cdot \left(\mathbf{u} \cdot \frac{1}{2}Z^2 \right) = \nabla \cdot \left(D\nabla \frac{1}{2}Z^2 \right) - \chi - Z(G \cdot \mathbf{u}), \quad (8)$$

where $\chi = 2D \|\nabla Z\|^2$ is the scalar dissipation rate. When Eq. 8 is averaged, only the scalar dissipation rate and the forcing term retain non-zero values, as the scalar fluctuations, Z , must vanish, and stationarity forces the time derivative to zero. This leaves Eq. 9,

$$\langle \chi \rangle = -G \cdot \langle \mathbf{u}Z \rangle, \quad (9)$$

which mandates that the scalar flux in the direction of the mean scalar gradient assume a non-zero value. Thus, any scalar field derived from a mean scalar gradient forcing can never attain isotropy. Furthermore, this scalar forcing scheme only maintains statistical stationarity because it is anisotropic. In other words, it is the anisotropy that prevents the scalar field from decaying. Additionally, this forcing mechanism can only be used for passive scalars. With an active scalar, the anisotropy that is methodically maintained in the scalar field would have the opportunity to inject itself into the velocity field, corrupting its isotropy. In this instance, the mean scalar gradient forcing would not be an ideal candidate for the study of HIT.

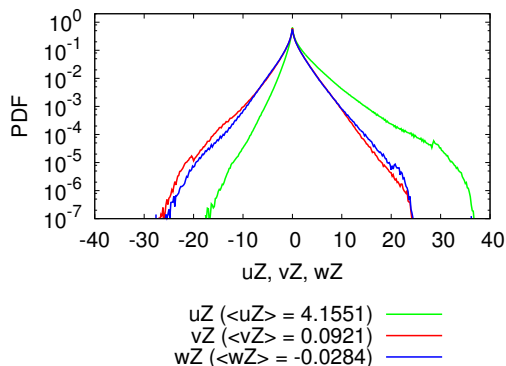


Figure 7: PDF of scalar flux obtained using a mean scalar gradient forcing and the spectral velocity forcing ($N = 512^3$, $Re_\lambda = 140$, $Sc = 1$).

3.2 DERIVATION OF NEW FORCING TECHNIQUE

The development of this new scalar variance forcing was motivated by the linear velocity forcing of Lundgren [10], its successful implementation [11], and the non-idealities associated with the established mean scalar gradient forcing previously discussed. This new proposed scheme aims to create a scalar field subject to constant scalar energy. In a turbulent flow, at every timestep, n , the scalar quantity, Z^n , will have an associated scalar energy, or variance, Z_V^n . After convection, the scalar field will have a new variance value, Z_V^* , where, $Z_V^* \neq Z_V^n$. To simulate sustained, decaying grid turbulence, the variance must be constrained to be constant at each timestep. Let this constant variance be called α . To accomplish this, the scalar field is rescaled at each step, $(n + 1)$, according to

$$Z^{n+1} = Z^* \sqrt{\frac{\alpha}{Z_V^*}}. \quad (10)$$

If $Z_V^* = \alpha$, then $Z^* = Z^{n+1}$; otherwise, the scalar quantity at the subsequent timestep, Z^{n+1} , is either increased or decreased. An increase in Z^{n+1} will result in a larger calculated variance, Z_V^* ; a decrease will result in a smaller Z_V^* . To derive the source term for the scalar equation, consider the variance equation,

$$\frac{\partial Z_V^*}{\partial t} = -\chi. \quad (11)$$

Integrating Eq. 11 discretely admits $Z_V^* = Z_V^n - \chi\Delta t$, such that Eq. 10 can be expanded to the form,

$$Z^{n+1} = Z^* \sqrt{\frac{\alpha}{Z_V^n - \chi\Delta t}}. \quad (12)$$

Using Taylor-expansion to first-order for small timesteps, Δt , Eq. 13 is obtained.

$$Z^{n+1} \approx Z^* \sqrt{\frac{\alpha}{Z_V^n}} \left(1 + \frac{1}{2} \frac{\chi\Delta t}{Z_V^n} \right) \quad (13)$$

The discrete version of the decay rate of a scalar quantity, $\frac{\partial Z}{\partial t}$, can be expressed as,

$$\frac{\partial Z}{\partial t} \approx \frac{1}{\Delta t} (Z^{n+1} - Z^n) \approx \frac{1}{\Delta t} (Z^{n+1} - Z^* + Z^* - Z^n). \quad (14)$$

Utilizing Eq. 13, allows the rate of scalar decay to be approximated as,

$$\frac{\partial Z}{\partial t} \approx Z^* \left(\frac{1}{\Delta t} \left(\sqrt{\frac{\alpha}{Z_V^n}} - 1 \right) + \frac{1}{2} \sqrt{\frac{\alpha}{Z_V^n}} \frac{\chi}{Z_V^n} \right) + \frac{1}{\Delta t} (Z^* - Z^n). \quad (15)$$

The first term on the right-hand side represents the rescaling to preserve a constant variance. The second term represents the change in the scalar due to both convective and diffusive transport. Assuming the rescaling between two timesteps is small, the two fields Z^* and Z^n are very similar ($Z^* \approx Z^n$), and the two variances are almost identical ($Z_V^n \approx \alpha$), then this proposed forcing technique takes the form,

$$\frac{\partial Z}{\partial t} + \mathbf{u} \cdot \nabla Z = D\nabla^2 Z + \left[\frac{1}{\tau_I} \left(\sqrt{\frac{\alpha}{Z_v}} - 1 \right) + \frac{1}{2} \frac{\chi}{Z_v} \right] Z. \quad (16)$$

where Z_v , χ , and $\frac{1}{\tau_I}$ are the scalar variance, scalar dissipation rate, and an inertial relaxation timescale, respectively.

The proposed forcing function is composed of a relaxation term $\left(\frac{1}{\tau_I} \left(\frac{1}{\sqrt{Z_v}} - 1 \right) \right)$ and a production term $\left(\frac{\chi}{Z_v} \right)$. The relaxation term allows the field to evolve towards a specified variance, or average scalar energy, while the production term is designed to balance exactly any losses from dissipation. This scheme has the advantage of being mathematically isotropic and statistically stationary. In addition, the forcing preserves the linearity of the original, unforced scalar transport equation with respect to the scalar quantity.

3.3 PHYSICAL SIGNIFICANCE AND CONTRAST WITH MEAN SCALAR GRADIENT FORCING TECHNIQUE

The connection of this scalar variance forcing scheme to the physics of a decaying scalar in a turbulent flow can be made by considering a turbulent field generated via the motion of a heated grid, as investigated in [7], [8], and [9]. In these experiments, a grid is forced through a fluid with a pre-existent scalar distribution. The passage of the grid serves as the only means of energy injection into the velocity and scalar fields. Once the grid has passed, a transient turbulent flow is established, which will evolve into a self-similar regime. This self-similar regime is characterized by a velocity field that is statistically stationary and a decaying scalar field. When appropriately scaled, the scalar energy spectra of the self-similar region can be collapsed to a single curve. The scalar field can be represented in terms of the scalar variance, $Z_V = \langle Z^2 \rangle - \langle Z \rangle^2$. The proposed scalar forcing mimics this self-similarity by, at every time step, scaling the scalar by its standard deviation. This is numerically equivalent to a physically self-similar flow regime. In this sense, this forcing technique should be able to reproduce the physics of a decaying scalar field embedded in a turbulent velocity field. The mean scalar gradient forcing technique stands in contrast with the proposed forcing. The constant presence of a mean gradient across the scalar field serves as a reservoir for continuous energy injection into the scalar field.

4 VALIDATION OF THE VARIANCE FORCING TECHNIQUE

As stated previously, an objective of this study was to simulate correctly the physics of a decaying turbulent scalar field for a sufficiently long time in the absence of an imposed scalar gradient. The simulations listed in Table 1 consisted of a spectrally-forced velocity field and the scalar variance forcing previously presented. The validation of this methodology took the following form. First, the PDFs of the scalar flux for each simulation were calculated. To be representative of a symmetric and isotropic decay, the scalar flux must be symmetric and centered at a mean value of zero. Second, the spectra are examined. For each Sc , the spectra generated from the scalar variance forcing were compared to spectra from the decay of a statistically stationary scalar field; the convergence of these spectra provide confirmation that the use of this scalar variance forcing method will reproduce the physics associated with a decaying scalar field.

4.1 RESOLUTION

Prior to discussing the results of the simulation study, a brief discussion of the operating conditions of the simulations will be provided. The resolution requirements for any DNS study is $\kappa\eta \geq 1.5$ for the velocity field [3] and $\kappa\eta_b \geq 1.5$ for the scalar field [4]. These restrictions make the simulation of high-Schmidt number scalars computationally expensive. In a previous work, we have developed a method for the simulation of high-Schmidt number scalar mixing, referred to as SF-DNS [13]. Here, only a brief description is provided. This methodology relies on the observation that the velocity spectrum will decay much more rapidly than the corresponding scalar field, as depicted in Fig. 8. In SF-DNS, the scalar field is spectrally filtered; all scalar quantity information associated with sufficiently high wavenumbers, κ , is deleted.

The justification for utilizing filtered scalar fields in DNS studies can be understood by consideration of the advection-diffusion equation, Eq. 2. If the advection-diffusion equation is filtered by any homogeneous spatial filter, Eq. 17 results.

$$\frac{\partial \tilde{Z}}{\partial t} + \nabla \cdot (\tilde{u}\tilde{Z}) = \kappa \nabla^2 \tilde{Z} - \nabla \cdot (\tilde{u}\tilde{Z} - \tilde{u}\tilde{Z}) \quad (17)$$

In Eq. 17, the final term is commonly called the sub-grid scalar flux (SGF) term. It is this term which represents the impact the smallest scales have on the larger, super-grid scales.

As the velocity fluctuations at the smaller scales, such as those where $\kappa\eta \geq 3$ in Fig. 8, have vanishingly small energy content, the filtered velocity field, \tilde{u} , can be assumed to be energetically equivalent to the full, unfiltered velocity field, u . More concisely, the velocity field can be assumed invariant with respect to the filtering operation such that $u \approx \tilde{u}$. Thus, the SGF can be rewritten as, $u\tilde{Z} - \tilde{u}\tilde{Z} \approx 0$. As a result, it is reasonable to state that the solution to the filtered advection-diffusion equation will recover a very close approximation to the full scalar field solution determined from all wavenumber data, despite the deletion of scalar field information for all wavenumbers larger than κ_{filter} . As long as the placement of the filtering wavenumber, κ_{filter} , is thoughtfully considered, the error introduced into the subsequent calculations will be minimal. Referring to Table 1, only simulations 5-7 would qualify as having a filtered scalar field; note that the velocity fields are completely resolved in these cases ($\kappa_{max}\eta \geq 1.5$).

4.2 SCALAR FIELD STATISTICS

To remain consistent with the physics of a real scalar decaying in a turbulent field, the scalar statistics must be isotropic and symmetric. To determine if the proposed forcing was able to reproduce these rather strict requirements, the probability density functions of scalar flux for each simulation were calculated. For all simulations listed in Table 1, only one representative scalar flux PDF is provided for each Sc (at $Re_\lambda = 55$), as the scalar flux data obtained for the other simulations had consistent statistical character. These scalar

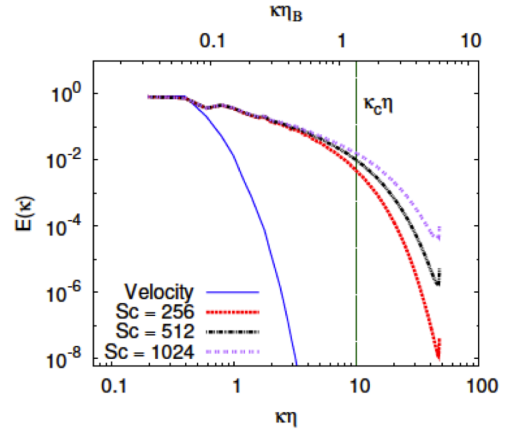


Figure 8: 3-D velocity ($\eta = 0.1958$) and scalar spectra for $Sc = 256, 512, 1024$ [12].

fluxes, which are averaged over two τ_{eddy} (b & c) or three τ_{eddy} (a & d), are depicted in Fig. 9. As is apparent in Fig. 9, the scalar fluxes are symmetrically distributed about a value of zero. The tails of the PDFs are indicative of almost perfect isotropy.

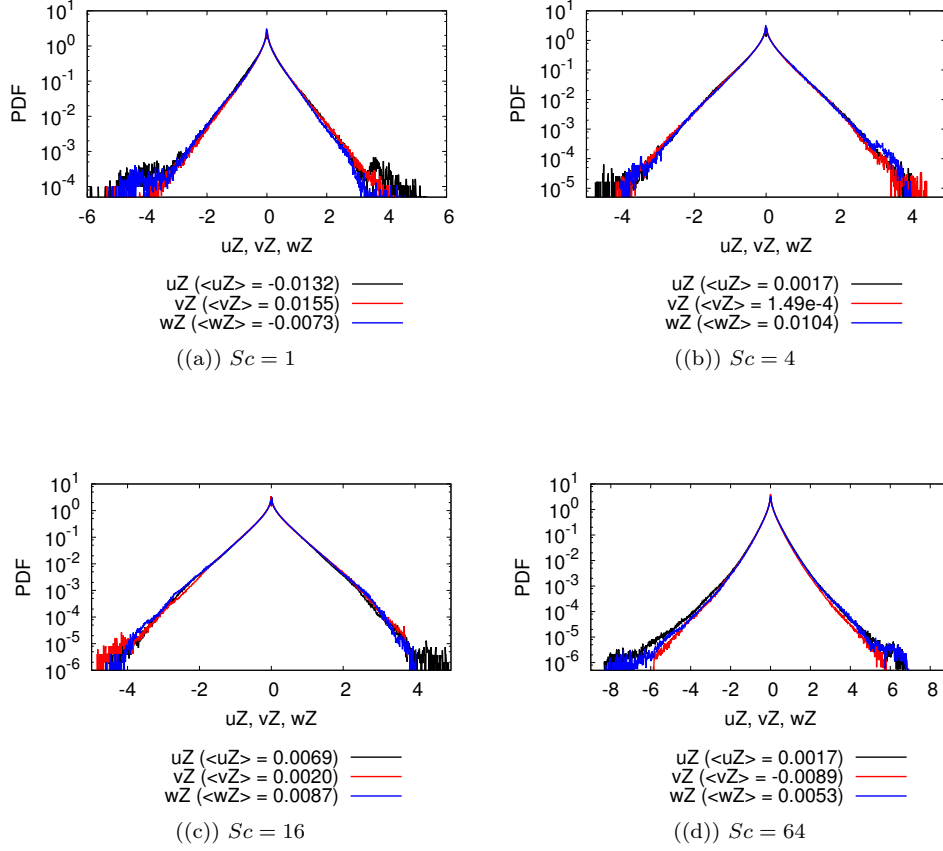


Figure 9: PDF of scalar flux for simulations conducted at $Re_\lambda = 55$ as listed in Table 1. These statistics are averaged over two τ_{eddy} (b & c) or three τ_{eddy} (a & d), where $\tau_{eddy} \approx 4$.

4.3 SCALAR FIELD ENERGY SPECTRA

With the scalar forcing reproducing the desired properties of homogeneity and isotropy, the scalar energy spectra were then calculated. As stated initially, the objective of this research effort is to create a framework to conduct simulations of decaying scalars subject to a turbulent flow. To ensure that the numerical scheme proposed is producing accurately the associated physics, the distinction between continuous energy injection and one-time energy injection is critical. A decaying scalar field is subject to energy injection only at $t = 0$. To produce a scalar energy spectrum specific to a decaying scalar field, we start with a statistically stationary scalar field that is subject to continuous energy injection, and then we turn off the forcing term, allowing it to decay. Examining the consistency between the scalar energy spectra obtained from the proposed scalar variance forcing and that from the decaying scalar field will indicate whether this proposed forcing method can reproduce the physics of turbulent scalar decay.

The mean scalar gradient forcing technique was used to create the initially statistically stationary scalar field. The spectra from the statistically stationary fields were calculated to ensure they were consistent with known scalar behavior. Then, these forced scalar fields were allowed to decay by deleting the source term in the scalar transport equation. The spectra for these decaying scalar fields were calculated at sequential eddy-turnover times, τ_{eddy} . With these data known, the scalar variance forcing was applied to a scalar field and the simulations were allowed to run until a statistically stationary state was obtained. Then, the scalar

spectra for this steady state were calculated. The comparison is done between the purely decaying spectra and the scalar variance-forced spectra.

This comparison was conducted for all simulations listed in Table 1. The results are shown only for $Re_\lambda = 55$ in Fig. 10; the other cases included in Table 1 produced similar results. In these figures, the black line shows the scalar energy spectrum that is obtained when the proposed scalar variance forcing is used to drive the scalar field to stationarity. The red line shows the scalar energy spectrum obtained when the mean scalar gradient forcing is used to force the scalar field to stationarity. It is this scalar field state which is allowed to decay. As a result, it is labeled as corresponding to $\tau_{eddy} = 0$. The blue line shows the scalar energy spectra obtained after the mean scalar gradient-forced scalar field is allowed to decay for the specified τ_{eddy} . As illustrated in Fig. 10, after an initial transient decay period, the decaying scalar fields converge to that predicted by the proposed scalar variance forcing for all Re_λ and Sc examined. It is of interest that, as the Sc was increased, the number of turn-over times required for convergence dropped, with the decaying scalar field assuming more rapidly a structure consistent with the spectrum generated by the scalar variance forcing scheme.

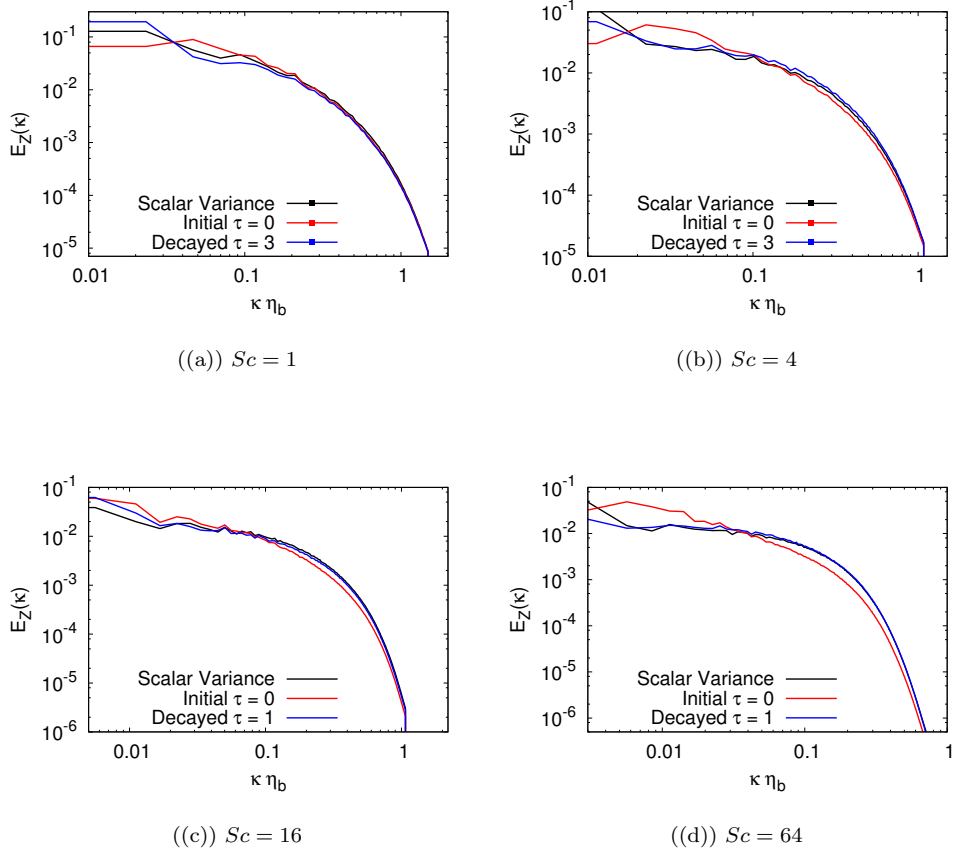


Figure 10: Evolution of a purely decaying scalar spectrum into the structure predicted by the scalar variance forcing method ($Re_\lambda = 55$).

5 CONCLUSIONS

The primary objective of this work was to develop a methodology for simulating the self-similar decay of a turbulent scalar and to offer commentary on the role of the velocity field in determining scalar field characteristics. The scalar variance forcing has been presented and the statistics produced by its implementation have been shown to reproduce the requirements of homogeneous isotropic turbulence. It has been demonstrated for the range of Sc considered in this study that the pure decay of a statistically stationary scalar field will evolve into the spectrum predicted by the scalar variance forcing. As presented, this methodology can be implemented to perform simulation studies of the decay of passive scalar quantities embedded in a turbulent environment.

References

- [1] P.K. Yeung. Schmidt Number Effects on Turbulent Transport with Uniform Mean Scalar Gradient. *Phys. Fluids*, 12:4178-4191, 2002.
- [2] D.A. Donzis, K.R. Sreenivasan, and P.K. Yeung. The Batchelor Spectrum for Mixing of Passive Scalars in Isotropic Turbulence. *Flow Turbulence Combust.*, 85:549-566, 2010.
- [3] S.B. Pope. *Turbulent Flows*. Cambridge University Press. 2000.
- [4] D.A. Donzis and P.K. Yeung. Resolution Effects and Scaling in Numerical Simulations of Passive Scalar Mixing in Turbulence. *Physica D*, 239:1278-1287, 2010.
- [5] K. Alvelius. Random Forcing of Three-Dimensional Homogeneous Turbulence. *Phys. Fluids*, 11:1880-1889, 1999.
- [6] G.K. Batchelor. Small-scale Variation of Convected Quantities like Temperature in Turbulent Fluid. 1. General Discussion and the Case of Small Conductivity. *J. Fluid Mech.*, 5:113-133, 1959.
- [7] R.A. Antonia. Effect of Schmidt Number on Small-scale Passive Scalar Turbulence. *Appl Mech Rev.*, 56:615-635, 2003.
- [8] R.A. Antonia, R.J. Smalley, T. Zhou, F. Anselmet, and L. Danaila. Similarity Solution of Temperature Structure Functions in Decaying Homogeneous Isotropic Turbulence. *Phys. Rev. E*. 69:1-11, 2004.
- [9] Jayesh, C. Tong, and Z. Warhaft. On Temperature Spectra in Grid Turbulence. *Phys. Fluids*. 6: 306-312, 1993.
- [10] T. Lundgren. Linearly Forced Isotropic Turbulence. *Center for Turbulence Research. Annual Research Briefs*. 2003.
- [11] C. Rosales and C. Meneveau. Linear Forcing in Numerical Simulations of Isotropic Turbulence: Physical Space Implementations and Convergence Properties. *Phys. Fluids*. 14 (095106), 2005.
- [12] P.K. Yeung, S. Xu, D. Donzis, and K. Sreenivasan. Simulations of Three-Dimensional Turbulent Mixing for Schmidt Numbers of the Order 1000. *Flow, turbulence and combustion* 72: 333-347, 2004.
- [13] S. Verma, P.K. Yeung, and G. Blanquart. Scalar Filtered - Direct Numerical Simulation (SF-DNS) Technique for Turbulent Transport of High Schmidt Number Passive Scalars. *Phys. of Fluids*. Submitted.
- [14] P.A. Durbin and B.A. Pettersson Reif. *Statistical Theory and Modeling for Turbulent Flows*. John Wiley & Sons, LTD. 2001.